Food Chemistry 390 (2022) 133145

Contents lists available at ScienceDirect

Food Chemistry

journal homepage: www.elsevier.com/locate/foodchem

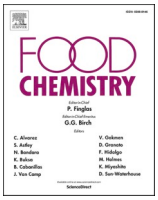

Quantitative assessment of epoxide formation in oil and mayonnaise by ^{1}H-^{13}C HSQC NMR spectroscopy

Vincent J.P. Boerkamp [a,1], Donny W.H. Merkx [a,b,c,1], Jianli Wang [a], Jean-Paul Vincken [a], Marie Hennebelle [a,*], John P.M. van Duynhoven [b,c]

[a] Wageningen University & Research, Laboratory of Food Chemistry, Bornse Weilanden 9, 6708 WG Wageningen, The Netherlands
[b] Unilever Food Innovation Centre, Bronland 14, 6708 WH Wageningen, The Netherlands
[c] Wageningen University & Research, Laboratory of Biophysics, Stippeneng 4, 6708 WE Wageningen, The Netherlands

ARTICLE INFO

Keywords:
Epoxides
Lipid oxidation
Bulk oil
Mayonnaise
HSQC NMR
Mechanistic insight

ABSTRACT

Lipid oxidation is detrimental for the quality of oil-based foods. Historically, lipid oxidation research focussed on hydroperoxides and aldehydes, but a third class, the epoxides, have been proposed to resolve observed mechanistic anomalies. Here, we developed a 2D ^{1}H-^{13}C HSQC NMR spectroscopic method to quantify epoxides in food in a reproducible (relative standard deviation $\leq$11.6 %) and sensitive (LoQ 0.62 mmol/kg oil) manner. Lipid hydroperoxides, aldehydes, and epoxides generated in rapeseed oil and mayonnaise were quantified over time by NMR. Epoxides accounted at most for 10–40 % of the products. They were formed after hydroperoxide accumulation, most likely primarily *via* alkoxyl radical intermediates, which limits their potential as an early oxidation marker. As 99 % and ~60 % of the epoxide signal intensities were assigned in a fatty acid and substructure specific manner, respectively, our quantitative HSQC method will enable unravelling and quantitative modelling of lipid oxidation mechanisms.

1. Introduction

Lipid oxidation is a concern for the shelf-life of many food products that are high in unsaturated fatty acids, such as vegetable oils and dressings. It is linked to the formation of off-flavours and, at later oxidation stages, to the physical destabilization of the food product. Lipid oxidation is classically described as a free radical chain reaction that can be divided in primary and secondary oxidation. In primary oxidation, a (bis)allylic hydrogen is abstracted, forming a resonance-stabilized radical that can react with O_2 to yield a peroxyl radical. This peroxyl radical can propagate the free radical chain reaction by abstracting a hydrogen from another fatty acid, forming lipid hydroperoxides (LOOHs). Secondary oxidation is the degradation of these hydroperoxides, which results in potent off-flavours such as aldehydes. This binary comprehension of the lipid oxidation mechanism has suited the industry and academia for a long period, but, in recent years, there has been an interest in more detailed assessment of the chemical mechanisms of lipid oxidation.

A major class of reaction products that has been often overlooked are the epoxides (Schaich, Xie, & Bogusz, 2017; Laguerre, Bily, & Birtić, 2020), which can be formed from peroxyl radicals during primary oxidation, or via alkoxyl radicals, the reactants of classical secondary oxidation (Schneider, Boeglin, Yin, Porter, & Brash, 2008). Epoxide generating mechanisms are dependent on environmental conditions such as temperature, oxygen availability, and protic solvent availability (Schaich et al., 2017). There is a growing interest in identifying and quantifying epoxides in lipid oxidation studies, since this may explain current unclarities in lipid oxidation mechanisms (Laguerre et al., 2020). Furthermore, there are reports that epoxides might be potential novel candidates as early marker of lipid oxidation in food (Grüneis & Pignitter, 2018). Currently, due to lack of rapid and quantitative methods, epoxides are rarely analysed in lipid oxidation studies, keeping their true impact and importance poorly understood. The official AOCS method (Cd 9–57) to quantify epoxides is a hydrogen bromide (HBr) titration with a low sensitivity and is influenced by the presence of conjugated dienes and molecular oxygen (Xia, Budge, & Lumsden, 2015). More recently, a liquid chromatography-mass spectrometry (LC-MS) method has been developed to detect epoxides and hydroperoxides

* Corresponding author.
E-mail address: marie.hennebelle@wur.nl (M. Hennebelle).
[1] Equal contributions.

https://doi.org/10.1016/j.foodchem.2022.133145
Received 18 February 2022; Received in revised form 22 April 2022; Accepted 1 May 2022
Available online 6 May 2022

simultaneously, unfortunately with a time consuming pre-concentration step that hampered the throughput (Grüneis et al., 2019). So far, a major impediment for unravelling the mechanistic role of epoxides and validating their use as early marker is the lack of simple and high-throughput quantitative methods.

In recent years, Nuclear Magnetic Resonance (NMR) spectroscopy has been shown to be a convenient tool to assess lipid oxidation products quantitatively and rapidly (Guillén & Ruiz, 2004; Guillen & Goicoechea, 2009; Skiera, Steliopoulos, Kuballa, Holzgrabe, & Diehl, 2012; Merkx, Hong, Ermacora, & van Duynhoven, 2018). It has been used to quantify epoxides in chemically oxidized and thermally autoxidized fatty acid esters and oil samples, when most double bonds are converted into epoxides (Goicoechea & Guillen, 2010; Xia et al., 2015; Xia, Budge, & Lumsden, 2016; Xia & Budge, 2017). When epoxides are obtained via autoxidation under moderate shelf-life conditions, the epoxide structures are more diverse, and their concentrations are orders of magnitude lower. This results in 1D spectra with significant overlap of the epoxide signals with each other and with unreacted bisallylic protons (Xia et al., 2016), which severely compromises quantification. A recourse for overcoming overlap in 1D NMR is the use of 2D NMR (van Duynhoven, van Velzen, & Jacobs, 2013).

Here, we propose the use of 2D heteronuclear single quantum coherence (HSQC) NMR spectroscopy to resolve the epoxide signals from each other and from the bisallylic signals. Whereas the signal area in 1D NMR spectra is solely dependent on the number of equivalent spins, this is not the case in HSQC. Due to differences in longitudinal/transversal relaxation times and homo-/heteronuclear coupling constants, the signal intensity is not inherently quantitative (Giraudeau, 2014; Fardus-Reid, Warren, & Le Gresley, 2016). To obtain quantitative results, one can modify the acquisition parameters to correct for heteronuclear coupling constants (Heikkinen, Toikka, Karhunen, & Kilpeläinen, 2003), determine a correction factor theoretically (Peterson & Loening, 2007), or determine a response factor empirically using samples with known analyte concentrations (Lewis et al., 2007). This last option will be further explored in this work.

In this paper, we describe the development of a novel 2D HSQC NMR method for identification and quantification of epoxides in real food systems, particularly rapeseed oil and mayonnaise. First, the method development and validation will be discussed. This 2D HSQC method will then be combined with a 1D quantitative NMR (qNMR) technique (Merkx et al., 2018) to comprehensively assess the formation of hydroperoxides, aldehydes, and epoxides under accelerated shelf-life conditions. We will evaluate the significance of epoxide generation as an early marker and discuss further mechanistic implications by varying the temperature (20, 40, and 60 °C) and sample matrix (rapeseed oil and mayonnaise).

2. Material and methods

2.1. Materials

Rapeseed oil and spirit vinegar were purchased from local suppliers. The rapeseed oil consisted of 68 % oleic, 17 % linoleic, 8 % linolenic, and 7 % saturated acid. Enzymatically modified egg yolk was obtained from Bouwhuis Enthoven (Raalte, the Netherlands). Sodium chloride, formic acid, hydrogen peroxide, ethyl acetate, triolein, trilinolein, and trilinolenin were purchased from Sigma Aldrich (Zwijndrecht, the Netherlands). Deuterated chloroform ($CDCl_3$) with 0.03 % tetramethylsilane (TMS), deuterated dimethylsulfoxide (DMSO-d_6), and deuterated 4 Å molsieves were purchased from Euriso-top (Saint-Aubin, France).

Stereochemistry is described using the *Z*, *E* notation when only carbon and hydrogen atoms were involved, e.g., to describe the configuration of double bonds, while the *cis*, *trans* notation was used when other atoms were involved, e.g., for epoxides.

2.2. Chemical epoxidation of rapeseed oil

Rapeseed oil was chemically epoxidized using formic acid and hydrogen peroxide, as described by Xia et al. (2016), which enabled the comparison between the 1D ^{1}H NMR and 2D ^{1}H–^{13}C HSQC spectra of epoxidized samples without bisallylic protons. In brief, formic acid and hydrogen peroxide were added to 3 mL fresh rapeseed oil in a molar ratio of 1:3:2 (formic acid:hydrogen peroxide:double bonds). The mixture was incubated under head-over-tail rotation for 16 h at 38 °C. Afterwards, the sample was mixed with 15 mL ethyl acetate and 22.5 mL saturated sodium chloride solution. The mixture was centrifuged (4,700x *g*, 5 min, 20 °C) and the epoxidized oil was recovered by drying the top (organic) layer under nitrogen flow at 30 °C.

2.3. Mayonnaise preparation

Mayonnaises were prepared by emulsifying rapeseed oil using a Silverson mixer (Silverson, Chesham, United Kingdom). Enzymatically modified egg yolk (5 % w/w) and sodium chloride (1.1% w/w) were mixed with demineralised water to obtain the aqueous phase (in total 20.6% w/w). Next, rapeseed oil (78 % w/w) was slowly added to form the emulsion, and finally spirit vinegar (1.4 % w/w) was added to achieve the desired pH (3.8).

2.4. Accelerated shelf-life experiments

For both the rapeseed oils and the mayonnaises, aliquots of 1 mL were stored in 20.4 mL clear headspace vials (internal diameter 20.5 mm) with screwcaps in the dark at 20, 40 and 60 °C. The samples were stored in a closed vial to limit the total amount of available O_2 and enable the determination of the O_2 consumption. To compare these results with lipid oxidation kinetics under unlimited oxygen supply, similar samples were also incubated in vials without a screwcap at an uncontrolled relative humidity. Samples were not agitated. The sampling frequency and total storage duration were based on the oxidation level of the samples, which depended on the sample matrix and storage conditions. The sampling of mayonnaise was ended as soon as phase separation was observed. All samples were stored at − 20 °C for at least 48 h prior to analysis. The headspace oxygen content was monitored with a MOCON OpTech-O_2 oxygen sensor (Ametek Mocon, Brooklyn Park, MN, USA). The initial amount of oxygen was calculated by using a 19.4 mL headspace volume with 20.9 % O_2 and 46.8 mg/kg oxygen concentration in the oil (Cuvelier, Soto, Courtois, Broyart, & Bonazzi, 2017).

2.5. NMR sample preparation

Chemically epoxidized and autoxidized rapeseed oil were used without modification. For the epoxide signal assignment, rapeseed oil, triolein, and trilinolein were stored at 60 °C for 16, 23, and 4 days, respectively, whereas trilinolenin was stored at 40 °C for 1 day. Triolein, trilinolein, and trilinolenin were selected as they represent the most abundant fatty acids present in vegetable oils. Mayonnaise samples were first freeze-thawed to break the emulsion and to yield a clean oil layer after centrifugation (15 min; 22,000x *g*; 20 °C). For both rapeseed oil and the oil layer of mayonnaise, 150 μL was dissolved in either 450 μL $CDCl_3$ (method development) or 5:1 $CDCl_3$:DMSO-d_6 (method development and shelf-life study), respectively, and transferred to 5-mm NMR tubes. Prior to sample preparation, the $CDCl_3$ and DMSO-d_6 were dried over deuterated 4 Å molecular sieves to remove residual water.

2.6. NMR acquisition

For the epoxide signal assignment, NMR spectra were recorded on a 950 MHz (22.3 T) Bruker Avance III NMR spectrometer (Bruker BioSpin, Switzerland) equipped with a cryo-probe. All other NMR measurements

were performed on a 600 MHz (14.1 T) Bruker Avance III NMR spectrometer (Bruker BioSpin, Switzerland) equipped with a cryo-probe. The internal temperature of the probe was set at 295 K. The 90° pulse length was determined automatically. The data was processed using either Bruker TopSpin v4.1.3 (Bruker BioSpin, Switzerland) or in MestReNova v14.1 (Mestrelab Research, S.L., Santiago de Compostela, Spain).

2.6.1. Epoxide signal assignment

A 2D ^{1}H–^{13}C HSQC spectrum was recorded using the standard "hsqcetgpsisp2.2" Bruker pulse sequence. In the ^{13}C-dimension, the spectral width was 200 ppm with an off-set of 80 ppm (δ_C 180 to − 20 ppm) and with 2048 increments. In the ^{1}H-dimension, the spectral width was 16 ppm with an off-set of 5 ppm (δ_H 13 to −3 ppm) with 16,384 increments. Sixteen scans were collected using a relaxation time of 1.2 to 1.5 s, and the INEPT delay set to an assumed $^{1}J_{CH}$ of 170 Hz. The standard "hsqcetgpml" Bruker pulse sequence was used to record 2D TOCSY-HSQC spectra. Three spectra were recorded which differed in mixing time (20, 50, and 80 ms), using the settings above, except for the number of increments that was set to 2048 and 8192 for the ^{13}C and ^{1}H-dimension, respectively. A TOCSY spectrum was recorded using the standard "mlevphpp" Bruker pulse sequence, 1024 and 8192 increments in the indirect and direct dimension, respectively, a spectral width of 16 ppm, and an offset of 5 ppm (δ_H 13 to −3 ppm). Sixteen scans were collected using a relaxation time of 2 s, and a mixing time of 80 ms.

For all experiments, zero-filling up to 8192 points was applied in the ^{13}C-dimension or indirect ^{1}H-dimension prior to Fourier transformation. In both dimensions, a squared sine window function with a sine bell shift of 2 was used. Phase and baseline correction were performed automatically, and the spectra were calibrated using TMS (δ_H 0 ppm, δ_C 0 ppm).

2.6.2. Quantification of epoxides

The standard "hsqcetgpsisp2.2" Bruker pulse sequence was used to record the 2D ^{1}H–^{13}C HSQC spectra. In the ^{13}C-dimension, the spectral width was 200 ppm with an off-set of δ 72.8 ppm (δ_C 172.8 to −27.2 ppm) and with 400 increments. In the ^{1}H-dimension, the spectral width was 4 ppm with an off-set of 3 ppm (δ_H 5 to 1 ppm) with 2048 increments. Two to twelve scans were collected using a relaxation time of 0.8 s. For the Fourier transformation in the ^{1}H-dimension, Gaussian apodization was used with a Gaussian max position of 0.001. For the ^{13}C-dimension, zero-filling up to 1024 points was applied prior to Fourier transformation with a squared cosine window function (SSB 2). Phase and baseline correction were performed automatically, and the upfield triacylglycerol (TG) backbone peak was calibrated to δ_H 4.13 ppm and δ_C 61.9 ppm. Integration was done automatically using predefined elliptical integration ranges in MestReNova v14.1. Details on the integrations can be found in Table S1. The concentration of epoxides was expressed in mmol/kg oil and calculated using Eq. (1) for the 1D experiment (for the chemically epoxidized oil samples) and Eq. (2) for the 2D HSQC experiment.

$$c_{epox}\,(mmol/kg) = \frac{I^{1D}_{epox}}{I^{1D}_{TG}} \bullet \frac{N_{TG}}{N_{Epox}} \bullet \frac{10^6}{MW_{TG}} \tag{1}$$

$$c_{epox}\,(mmol/kg) = \frac{I^{2D}_{epox}}{I^{2D}_{TG}} \bullet \frac{N_{TG}}{N_{epox}} \bullet \frac{10^6}{MW_{TG}} \bullet K \tag{2}$$

Here, I was the NMR signal integral, N the number of protons, and MW the molecular weight (average triglyceride ~ 880 g•mol^{-1}). Index 'epox' stands for epoxide, and 'TG' for triacylglyceride. The factor K was empirically determined and links the 1D response to the 2D response of both TG and epoxide moieties, as described in Eq. 4–7. The spectral integration region to determine I_{TG} was δ_H 4.4 to 4.0 ppm, with N_{TG} corresponding to the four outer protons of the TG backbone. The TG backbone was not expected to undergo changes upon oxidation, hence its methylene ^{1}H NMR signal was used as internal standard (Skiera et al., 2012). The integrals I_{epox} are determined from the spectral integration regions listed in Table S1, all with N_{epox} corresponding to 2. The proposed correction factor K was built on the theoretical constant k (Lewis et al., 2007) according to Eq (3). Combining Eq. (3) with Eq. (1) and Eq. (2) yielded Eq. 4–7. The assumption was made that the concentration (c) is proportional to the 1D-integral (I) divided by the number of protons (N).

$$V \text{ or } I^{2D} = k \bullet c \bullet N \bullet Vs \tag{3}$$

$$\frac{I^{2D}_{epox}}{I^{2D}_{TG}} = \frac{k_{epox}}{k_{TG}} \bullet \frac{c_{epox}}{c_{TG}} \bullet \frac{N_{epox}}{N_{TG}} \bullet \frac{Vs}{Vs} \tag{4}$$

$$\frac{I^{2D}_{epox}}{I^{2D}_{TG}} = \frac{k_{epox}}{k_{TG}} \bullet \frac{I^{1D}_{epox}}{I^{1D}_{TG}} \bullet \frac{N_{TG}}{N_{epox}} \bullet \frac{N_{epox}}{N_{TG}} \tag{5}$$

$$\frac{I^{2D}_{epox}}{I^{2D}_{TG}} = K \bullet \frac{I^{1D}_{epox}}{I^{1D}_{TG}}, \text{ where } K \equiv \frac{k_{epox}}{k_{TG}} \tag{6}$$

$$K = \frac{I^{1D}_{epox}}{I^{1D}_{TG}} \bullet \frac{I^{2D}_{TG}}{I^{2D}_{epox}} \tag{7}$$

Here, V or I^{2D} was the peak volume or 2D-integral, k is the HSQC-constant, c the concentration, N the number of protons, Vs the sensitive coil volume and K the combined epoxide-constant. The main requirement for the determination of K is that the epoxide and TG region can be accurately integrated in both 1D and 2D (HSQC) spectra. A K-factor of 1.16 was used in this research. Note that the K-factor is dependent on the experimental settings for both the 1D and 2D experiments.

2.6.3. Quantification of lipid hydroperoxides and aldehydes

Hydroperoxides and aldehydes were measured using single pulse and band selective ^{1}H NMR spectra and quantified using MestReNova v14.1. Details on signal assignment and quantification can be found in Merkx et al. (2018). For the quantification of *E,E*-LOOH and *Z,E*-LOOH from linoleic acid, the integration regions from δ_H 10.932 to 10.883 ppm and from 10.883 to 10.833 ppm were used, respectively.

2.7. Validation of epoxide quantification

The repeatability (r) and within-laboratory reproducibility (R) were determined by measuring three autoxidized oil samples in duplicate for four days (total 24 samples). The three epoxide concentrations that were assessed corresponded to anticipated levels during supply chain shelf-life conditions. The r and R for each concentration level were obtained using an ANalysis Of VAriance (ANOVA) model. Results were expressed as relative standard deviations of repeatability (RSD_r) and within-laboratory reproducibility (RSD_R). The limit of detection (LoD) and limit of quantification (LoQ) were respectively based on estimates of three and ten times the standard deviation divided by the average concentration from ten samples with an epoxide concentration lower than 1 mmol/kg. The trueness of epoxide quantification using ^{1}H NMR, which is required for the accurate determination of the K-factor, was previously shown by Xia et al. (2015).

3. Results and discussion

3.1. HSQC NMR spectral assignments of epoxide signals

To explore the scope of NMR for the quantification of epoxides in mildly oxidized food, fresh rapeseed oil (Fig. 1A/D/G) was both chemically epoxidized by a mixture of formic acid and hydrogen peroxide (Fig. 1B/E), and autoxidized (Fig. 1C/F/H). In chemically epoxidized rapeseed oil, the epoxide signals (δ_H 3.20 to 2.85 ppm) were baseline separated in the 1D spectrum, similar to those reported by Xia et al. (2015). Here, the absence of bisallylic signals (δ_H 2.85 to 2.70 ppm)

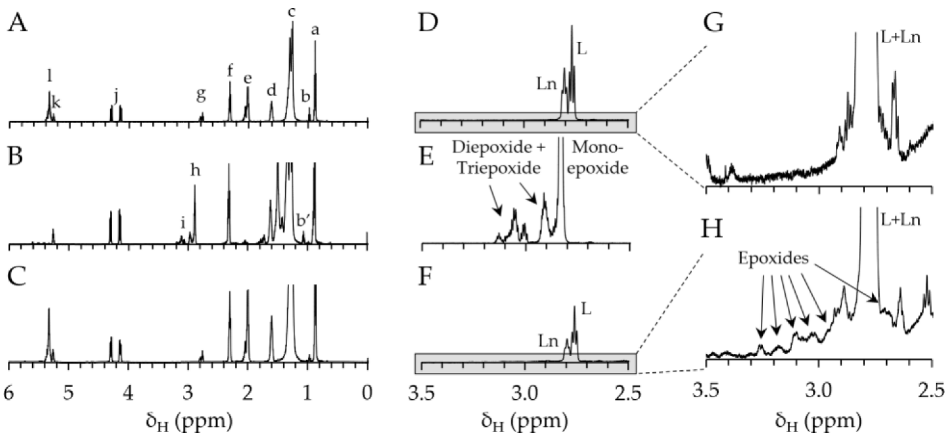

Fig. 1. ^{1}H NMR (600 MHz, $CDCl_3$) spectra of (A, D) non-oxidized rapeseed oil, (B, E) chemically epoxidized and (C, F) autoxidized rapeseed oil ([LOOH] = 200 mmol/kg). In panels G and H, zoomed in ^{1}H NMR spectra are shown of the epoxide region, large tails and ^{13}C satellite signals of the bisallylic hydrogens from linoleic acid (L) and linolenic acid (Ln) are observed. Spectral assignments of panel A-C can be found in Table S2.

showed that the double bonds were fully converted to the epoxide moieties. This observation was in stark contrast to strongly autoxidized rapeseed oil (Fig. 1C/F/H), where the bisallylic signals decreased only by 45 % compared to the fresh rapeseed oil. In the autoxidized sample, epoxides were indeed accumulating (Fig. 1H). Their quantification, however, was impossible using the 1D spectrum, due to overlapping bisallylic protons. Therefore, we investigated the possibility of using 2D HSQC to capitalize on the added resolution in the carbon dimension.

In the 2D HSQC spectrum of epoxidized oils (Fig. S1), a large number of epoxide crosspeaks (δ_C 70 to 40 ppm) were well separated from each other and from the bisallylic signal (δ_C 25.5 ppm), allowing for both peak assignment and quantification. The high number of signals (~60) in the epoxide region strongly overlap in the 1D ^{1}H NMR spectrum and can only be resolved and quantified by 2D HSQC.

The advantage of separating the signals in the ^{13}C dimension by HSQC was exploited to assign the epoxide signals in a fatty acid specific manner. Hereto, pure TAGs (triolein, trilinolein, and trilinolenin) were autoxidized and their HSQC spectrum was compared to autoxidized rapeseed oil. Based on their chemical shift, all the signals in the region between δ_H 3.48–2.68 ppm and δ_C 62–52 ppm of the HSQC spectrum were assigned to epoxides. Nearly all signals (>99 % of the intensity) in this region could be assigned to a parent fatty acid, and no epoxide signal corresponded to more than one parent fatty acid (Fig. 2). The assignment of the last < 1 % was hampered by low signal intensity and/or signal overlap.

The molecular sub-structures of the eight most predominant

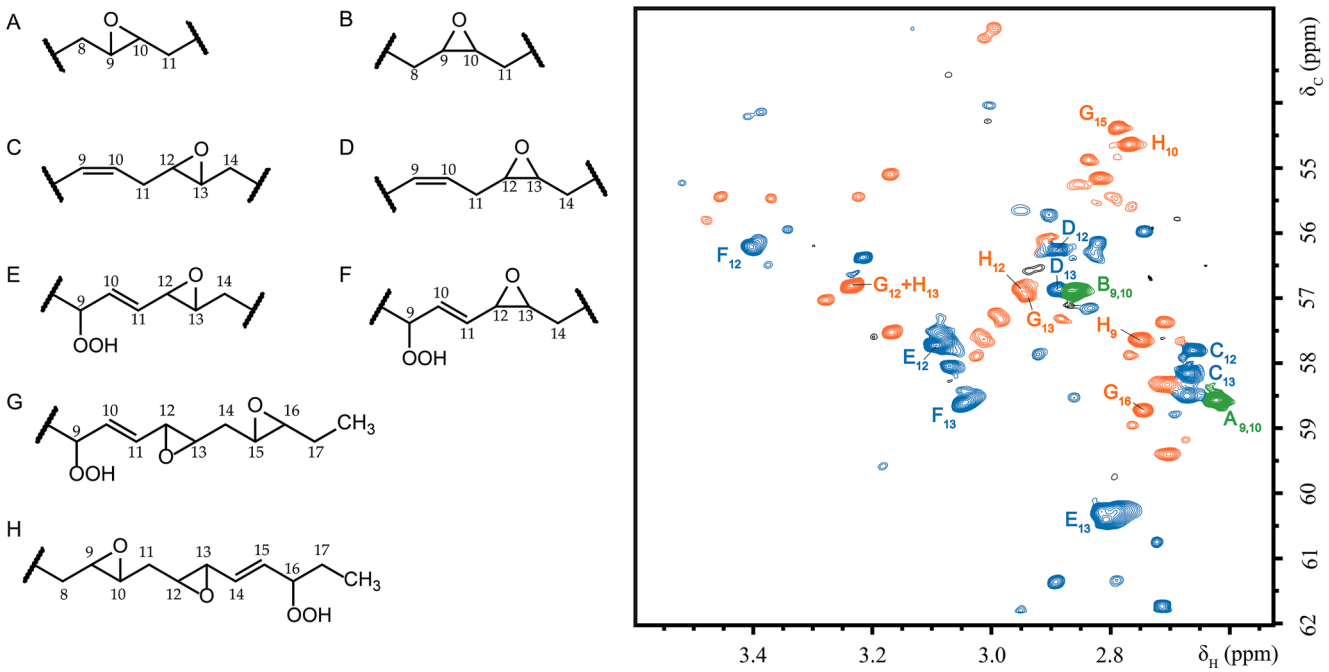

Fig. 2. Epoxide region in a 2D HSQC NMR spectrum (950 MHz, $CDCl_3$:DMSO-d_6, 5:1) of thermally autoxidized rapeseed oil (sixteen days at 60 °C) with the annotation of the eight most abundant peaks. The letters in the spectrum correspond to the structures next to the spectrum and the numbers to the carbon number. Epoxides derived from oleate, linoleate, and linolenate residues are coloured green, blue, and orange, respectively. Epoxides with an unassigned fatty acid parent are in black. The signals A and B were a group of mono-epoxides originating from oleate with the epoxide moiety on C8-C9, C9-C10, or C10-C11. The signals C-F were a combination of the drawn substructures, as well as the mirrored substructure with the epoxide at C9 and C10. They originated from linoleate, while signals G and H came from linolenate. The chemical shifts of the assigned epoxides are listed in Table S3 in the SI. (For interpretation of the references to colour in this figure legend, the reader is referred to the web version of this article.)

epoxides were assigned using additional 2D TOCSY and 2D TOCSY-HSQC experiments (details in Table S3) and confirmed by literature (Gardner, Weisleder, & Kleiman, 1978; Hidalgo, Zamora, & Vioque, 1992; Lin, Fay, Welti, & Blank, 1999; Schneider, Boeglin, & Brash, 2004; Lin, Zhang, & Sayre, 2007; Schneider et al., 2008; Nilewski, Chapelain, Wolfrum, & Carreira, 2015; Alberdi-Cedeño, Ibargoitia, & Guillén, 2020). These eight epoxides accounted for ~ 60 % of the total of epoxide HSQC signal integrals in rapeseed oil oxidized for sixteen days at 60 °C, the other epoxides were not annotated. Two annotated epoxides originated from oleic acid (18:1) and were *cis* and *trans*-monoepoxides flanked by alkyl groups (Fig. 2A, B). Four epoxides came from linoleic acid (18:2). They were *cis* and *trans* isomers of monoepoxides without alteration of the other double bond (Fig. 2C, D) and *cis* and *trans* isomers of monoepoxides connected *via* a double bond to a hydroperoxide, for instance 9-hydroperoxy-*trans*-12,13-epoxy-10*E*-octadecenoate (Fig. 2E, F). The same products have been observed in autoxidized omega-6 rich corn oil (Alberdi-Cedeño et al., 2020).

The signals annotated as G and H in Fig. 2 were assigned to oxidation products of linolenic acid (18:3) and exist as diepoxides with a double bond and hydroperoxyl moiety. The 2D HSQC-TOCSY and 2D TOCSY spectra used for the annotation are shown in the supplementary data in Fig. S2 and Fig. S3, respectively. The double bond configuration has been assigned tentatively to the *E* (entgegen) stereochemistry. These structures have, to the best of our knowledge, not been reported in literature on lipid autoxidation yet. A similar substructure has, however, been observed in the enzymatic biosynthesis of prostaglandin, using arachidonic acid (20:4, omega-6) as parent fatty acid (Schneider et al., 2004). Here, we propose a similar formation mechanism involving linolenic acid and two subsequent attacks by oxygen.

For the quantification of the total epoxide concentration in the following sections, we considered all epoxide signals in Fig. 2. See Table S1 for a list of the signal regions used for epoxide quantification.

3.2. Optimisation of quantitative epoxide assessment by HSQC

3.2.1. Acquisition parameters

Firstly, the spectral range in the ^{1}H dimension was optimized for quantitative coverage to include the epoxide signals and preferably an internal standard for quantification. We selected the triacylglyceride backbone CH_2-peaks (TG) as an internal standard, similarly to the 1D experiment to quantify the hydroperoxides and aldehydes (Merkx et al., 2018). The TG signals (δ_H 4.4 to 4.1 ppm) were well separated and relatively close to the epoxide signals in the HSQC spectrum (Fig. S1). We compared the quality of HSQC spectra recorded with spectral ranges in the ^{1}H dimension from δ_H 5 to 1 ppm and 9.5 to 0.5 ppm. The tighter spectral range (Fig. S4B) had improved resolution over the full spectral range (Fig. S4A). Hence, δ_H 5 to 1 ppm was selected as spectral width.

Next, the excited width in the ^{13}C dimension was narrowed by using selective pulses. These are typically used to overcome two problems: lack of resolution and dynamic-range limited sensitivity. An improved peak resolution for equal measurement time was obtained when using selective ^{13}C pulses (Fig. S4C). However, since for our application, no sensitivity improvement was observed, we chose the more accessible and widely used regular HSQC pulse sequence. To further reduce the measurement time, non-uniform sampling (NUS) was explored. NUS resulted in a loss in sensitivity (data not shown), and was therefore not further pursued.

3.2.2. NMR solvent selection

In our previous work, a solvent mixture comprising of five units $CDCl_3$ and one unit DMSO-d_6 (v/v) was used to shift the ^{1}H NMR signals of hydroperoxides downfield to an isolated spectral region, allowing accurate quantification and identification (Merkx et al., 2018). For simultaneous detection of hydroperoxides, aldehydes, and epoxides, it is convenient if the quantitative 2D HSQC approach works in this solvent system as well, without loss in sensitivity or the introduction of troublesome signal shifts. When comparing $CDCl_3$ to the mixture of $CDCl_3$ and DMSO-d_6 in a dilution series of epoxides ranging from 0.2 to 2 mmol epoxides/kg oil, no significant differences were found between the epoxide concentrations ($p > 0.05$) (Fig. S5). This implied that both the $CDCl_3$:DMSO-d_6 mixture as well as $CDCl_3$ could be used depending on the analyst's needs.

3.2.3. Determination of the K-factor

As mentioned before, HSQC is not inherently quantitative since the signal peak volume is influenced by transversal and longitudinal relaxation times as well as J_{CH} and J_{HH} coupling constants. These factors can be accounted for by a theoretical constant k, as described by Giraudeau (2014), but were difficult to determine experimentally for the signals of the glycerol backbone and epoxides. In this study, we opted for a combined empirical K-factor, which was used for direct quantification from the 2D HSQC spectrum (Eq. (2)). This K-factor was determined by quantitative comparison of the 1D signal integral and analogous 2D volume of the glycerol backbone and epoxide HSQC signals. Hereto, the epoxide signals needed to be baseline-separated in both the 1D and 2D spectra. Hence, rapeseed oil was chemically epoxidized by a mixture of formic acid and hydrogen peroxide until > 99 % of the double bonds were converted to epoxides (Fig. 1B and Fig. S1B). We assumed the K-factor in chemically epoxidized oil to be equal to that in thermally autoxidized oil. Moreover, the K-factor was assumed to be equal for all epoxide sub-classes regardless of their chemical structure. Henceforth, a K-factor of 1.16 was used in this study.

3.2.4. Experimental validation and duration

After determining the K-factor, the precision was determined by performing duplicate NMR experiments over different days. The fully chemically epoxidized rapeseed oil was diluted using fresh rapeseed oil to obtain three epoxide concentrations. The results were analysed by ANOVA and expressed in terms of repeatability and reproducibility (respectively between- and within-day variation) (Table 1). The repeatability and reproducibility were close, indicating that error on within-day duplicates is similar to the between-day repetitions. The limit of quantification of individual epoxide signals was 0.6 mmol/kg oil for an experimental duration of 70 min. Considering that typical shelf-life studies of food emulsions readily generate oxidation products above 2–5 mmol/kg, the measurement time of the HSQC-experiment can be reduced to less than twenty minutes by decreasing the number of scans. When the whole epoxide region (δ_C 61.3 to 52.3 ppm; δ_H 3.44 to 2.38 ppm) was integrated instead of individual signals, the limits of detection and quantification were an order of magnitude higher (LoD 2.2 mmol/kg). So, if the epoxide concentration is expected to be below this limit, it is advised to integrate the epoxide signals individually according to Table S1.

3.3. Formation and fate of epoxides during autoxidation of rapeseed oil and mayonnaise

The optimized and validated method was applied to assess the

Table 1
Validation results for the epoxide quantification using ^{1}H–^{13}C HSQC NMR (600 MHz, $CDCl_3$:DMSO-d_6, 5:1). The limit of detection (LoD) and limit of quantification (LoQ) were respectively based on 3 or 10 times the standard deviation divided by the average concentration from ten samples with an epoxide concentration lower than 1 mmol/kg oil. The repeatability (RSD_r) and reproducibility (RSD_R) were determined at three epoxide concentrations.

Epoxide conc. (mmol/kg)	RSD_r (%)	RSD_R (%)	LoD (mmol/kg)	LoQ (mmol/kg)
14.5	0.7	1.2		
1.35	4.1	4.0	0.19	0.62
0.53	8.2	11.6		

importance of epoxides in accelerated shelf-life tests of relevant food products. Rapeseed oil and mayonnaise were stored at 20, 40, and 60 °C in closed vials. Their hydroperoxide, aldehyde, and epoxide concentrations were followed over time by NMR spectroscopy.

At 20 and 40 °C, both in rapeseed oils and mayonnaises, the total oxygen consumption corresponded well with the sum of hydroperoxides, epoxides, and aldehydes (Fig. S6a,b,d,e). This indicated that these were the dominant oxidation products and that concentrations of compound classes like alcohols were minor. At 60 °C, the oxygen consumption agreed with the formation of these oxidation products in the early phase. However, after the lipid oxidation rate accelerated, the oxygen consumption was 40 to 60 mmol/kg higher than the total amount of detected oxidation products (Fig. S6c,f). This difference was attributed to an alternative fate of the alkoxyl radicals, such as polymer formation or reactions with proteins in mayonnaise that were not accounted for in the current quantitative NMR measurements. Moreover, our method did not account for potential loss of volatiles, such as aldehydes, which resulted in an underestimation of their concentrations.

The generation of all oxidation products, in both rapeseed oil and mayonnaises, was accelerated when increasing the storage temperature (Fig. 3). Mayonnaise had a lower oxidative stability with no observable initial lag phase. Epoxides and aldehydes followed hydroperoxide formation kinetics more closely in mayonnaise than in oil, which is attributed to the high interfacial area and abundance of iron in the emulsion systems. Iron is a pro-oxidant that catalyses the degradation of hydroperoxides by Fe(II) to form alkoxyl radicals and Fe(III) in a redox cycle (Berton-Carabin, Ropers, & Genot, 2014). The accelerated formation of alkoxyl radicals resulted in an earlier onset time as well as increased formation rate of aldehydes and epoxides. A similar trend was observed when increasing the storage temperature. At higher temperatures, the degradation of hydroperoxides to alkoxyl radicals was accelerated, which resulted in relatively more epoxides and aldehydes compared to hydroperoxides.

Under all conditions, hydroperoxides were the most abundant lipid oxidation product. Their concentration stayed an order of magnitude higher than that of epoxides and aldehydes, especially in the early stage of oxidation (Fig. 3, see Fig. S7 for linear y-scale). A similar trend was described by Xia et al. (2015) in a storage test of soybean oil at 100 °C and by Alberdi-Cedeño et al. (2020) for corn oil at 70 °C.

To look into more detail at the formation of epoxides, the main hydroperoxides and epoxides in bulk oil were quantified. For this purpose, rapeseed oil was oxidized under unlimited oxygen supply at 40 °C. Here, only the oxidation products of linoleic acid residues are discussed to reduce the complexity of the results. The first observed oxidation products were *E,Z*-LOOHs, followed by *E,E*-LOOHs (Fig. 4). The latter could be formed at an accelerated rate due to the decrease of hydrogen donors, such as naturally present anti-oxidants (Laguerre et al., 2020; Hoppenreijs, Berton-Carabin, Dubbelboer, & Hennebelle, 2021).

After around 62 days, we observed an acceleration in oxidation rate, which could be attributed to hydroperoxides reaching a critical concentration level at which association colloids (inverse micelles) were formed (Villeneuve, Bourlieu-Lacanal, Durand, Lecomte, McClements, & Decker, 2021). Concomitantly, epoxides and aldehydes were generated at a similar onset time (Figs. 3 and 4). As alkoxyl radicals are the main precursor of aldehydes (Laguerre et al., 2020), the results indicated that epoxides had also predominantly alkoxyl radical precursors. Such alkoxyl radicals can cyclize intramolecularly to epoxyl radicals (Gardner et al., 1978). These radicals can act as a chain carrier by either abstracting a hydrogen or by reaction with molecular oxygen. More epoxides with a hydroperoxyl moiety (Fig. 4E, F) were observed than without hydroperoxyl moiety (Fig. 4C, D), which indicated that, for linoleic acid, the epoxyallylic radical preferred reacting with oxygen over abstracting a hydrogen.

The concentration of epoxides with a hydroperoxyl moiety (E, F) decreased after 90 days, presumably due to the degradation of the hydroperoxyl moiety, which propagated further lipid oxidation. The epoxide ring itself appeared stable, as the concentration of epoxide substructures without a hydroperoxyl moiety (Fig. 4C, D) was constant after 100 days. Similar trends were observed under limited oxygen conditions (Fig. S8), albeit at a much lower epoxide concentration due to the limited oxygen supply.

During early stage of oxidation, most oxidation products were derived from linoleic and linolenic acid (Fig. S9), as expected from their oxidative stability relative to oleic acid (Holman & Elmer, 1947). In the late stage, oxidation products of oleic acid became dominant, as the monoepoxides were stable in our systems, even under unlimited oxygen supply. Interestingly, limiting the oxygen supply changed the stereospecificity of monoepoxide formation. Under unlimited supply of oxygen, a racemic mixture of *cis* and *trans*-epoxides was obtained, while when molecular oxygen was depleted, fewer *trans*-epoxides were generated (Fig. S10). In follow-up work, we will investigate the chemical significance of this observation.

All the above results showed that epoxides were generated after the accumulation of hydroperoxides with a similar onset time as for aldehydes. As aforementioned, these results indicated that epoxides derived predominantly from alkoxyl radical intermediates, similarly to the aldehydes (Fig. 5). Since the concentration of epoxides was higher than that of aldehydes, alkoxyl radicals would preferably form epoxides over

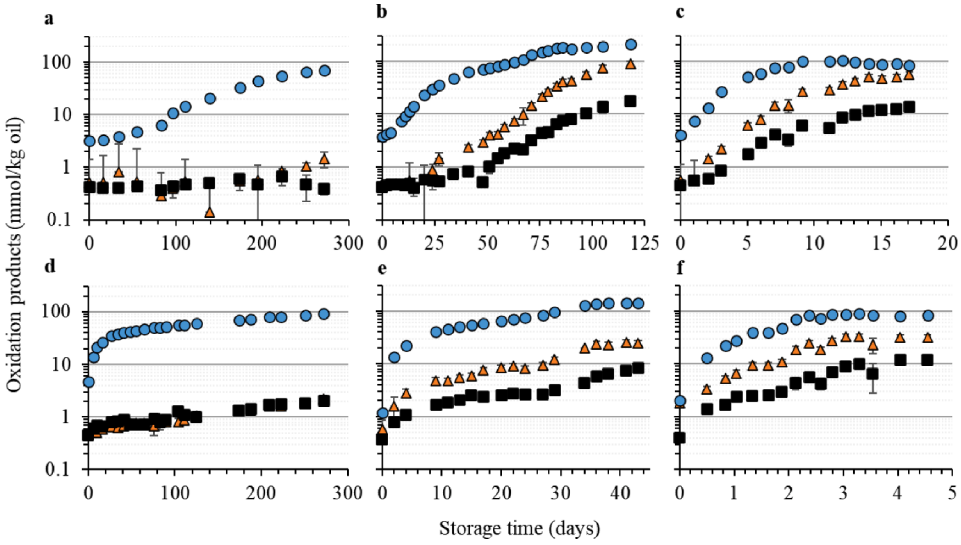

Fig. 3. Formation of lipid hydroperoxides (blue circles), epoxides (orange triangles) and aldehydes (black squares). Panels a-c correspond to rapeseed oil stored at 20, 40, and 60 °C, respectively. Panels d-f correspond to mayonnaise stored at 20, 40, and 60 °C, respectively. The error bars display the standard deviation, in case no error bars are visible, they are hidden below the marker. The epoxide concentration is base on the sum of all epoxide signals (Table S1). Note the logarithmic scale on the y-axis. (For interpretation of the references to colour in this figure legend, the reader is referred to the web version of this article.)

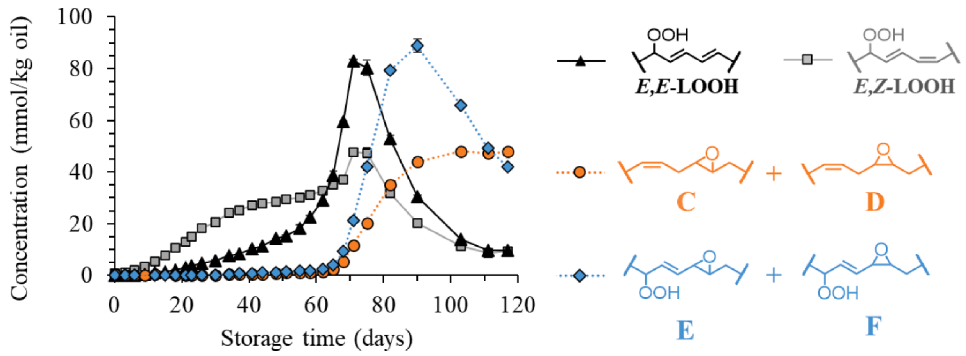

Fig. 4. Formation of oxidation products from linoleic acid (18:2) in bulk rapeseed oil stored at 40 °C under unlimited oxygen supply (uncontrolled relative humidity, ~10 %). The solid lines (LOOH) and dotted lines (epoxides) were added to guide the eye. Epoxide structures were annotated conform to Fig. 2. See Fig. S8 for an equivalent figure under limited oxygen supply.

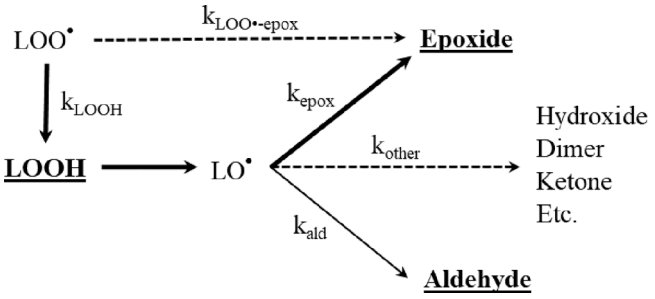

Fig. 5. A schematic interpretation of the results, illustrating the possible pathways to form epoxides. In this study, the bold and underlined compounds were quantified. The terms 'k' represents a qualitative interpretation of the kinetics as lumped rate constants. In both rapeseed oil and mayonnaise, we observed for the hydroperoxyl radical ($LOO^{\bullet}$) $k_{LOOH} \gg k_{LOO\bullet \rightarrow epox}$ and for the alkoxyl radical ($LO^{\bullet}$) $k_{epox} > k_{ald} > k_{other}$.

aldehydes ($k_{epox} > k_{ald}$). Our results did not sustain formation of substantial quantities of epoxides directly from peroxyl radicals ($k_{LOO\bullet\text{-}epox}$), but did not exclude it. To be able to use epoxides as an early marker, their formation would need to be in competition with that of hydroperoxides (*via* peroxyl radicals, $k_{LOO\bullet\text{-}epox}$) rather than that of aldehydes (*via* alkoxyl radicals, k_{ald}), which was not the case in our systems.

Our results also showed that in bulk oil and model emulsions, epoxides were an oxidation product with a major contribution (10–40 %) to the oxygen mass balance in the later stages of the oxidation. Therefore, a combination of hydroperoxides, epoxides, and aldehydes, is essential to assess the relative contributions of the pathways mapped in Fig. 5. In future studies, this should provide a more comprehensive mechanistical view on lipid oxidation than either one of these product classes alone.

4. Conclusion

Two-dimensional heteronuclear single quantum coherence (HSQC) NMR can be used to quantify lipid epoxides in autoxidized oil-based food systems. HSQC does not suffer from the significant signal overlap that complicates quantification by 1D spectra. Epoxides were assigned in a fatty acid specific (>99 % of the total signal integral in the epoxide region of the HSQC spectrum) and sub-structure (~60 %) manner. Using a fully automated acquisition and processing workflow, a high reproducibility (RSD ≤ 11.6%) and sensitivity (LoQ 0.62 mmol/kg oil) was achieved. The method is compatible with simultaneous quantification of hydroperoxides and aldehydes, and therefore, enables unravelling the impact of storage conditions in different matrices on a compound class (hydroperoxides, epoxides, aldehydes) level.

Epoxides account for 10–40 % of the total oxidation products in bulk rapeseed oil and mayonnaise oxidized under mild conditions (≤60 °C). They appear to be primarily formed *via* alkoxyl radical intermediates, which limits their potential as an early oxidation marker. Epoxides are, however, an important complementary marker for secondary lipid oxidation since they seem to compete over the alkoxyl radical with aldehydes. Epoxide formation likely explains the low amount of lipid alcohol formation from alkoxyl radicals. The combination of comprehensive hydroperoxide, epoxide, and aldehyde quantification facilitates a deeper understanding into lipid oxidation and enables quantitative mechanistic modelling.

CRediT authorship contribution statement

Vincent J.P. Boerkamp: Conceptualization, Methodology, Investigation, Validation, Writing – original draft. **Donny W.H. Merkx:** Conceptualization, Methodology, Investigation, Validation, Writing – original draft. **Jianli Wang:** Methodology, Investigation. **Jean-Paul Vincken:** Supervision, Writing – review & editing. **Marie Hennebelle:** Conceptualization, Supervision, Writing – review & editing. **John P.M. van Duynhoven:** Conceptualization, Supervision, Writing – review & editing, Funding acquisition.

Declaration of Competing Interest

The authors declare the following competing financial interest(s): Donny W.H. Merkx and John P.M. van Duynhoven are employed by a company that manufactures and markets food products, such as dressings and mayonnaises.

Acknowledgements

We are grateful to Yanzhang Luo, Niels de Roo, and Ruud Aspers for their expert advice and assistance with the NMR experiments. We thank Christiaan Beindorff for his help with the quantification of the headspace oxygen content. Katharina Duran, Natalia Hutnik, and Lorenz Plankensteiner are thanked for their assistance in taking samples. The MAGNEFY facility at Wageningen University and the NMR Facility at Radboud University (both part of the Dutch national uNMR-NL facility) are gratefully acknowledged for the access to their NMR instruments. This research received funding from the Netherlands Organisation for Scientific Research (NWO) in the framework of the Innovation Fund for Chemistry (grant number 731.017. 301) and from the Ministry of Economic Affairs in the framework of the "TKI/PPS-Toeslagregeling".

Appendix A. Supplementary data

Supplementary data to this article can be found online at https://doi.org/10.1016/j.foodchem.2022.133145.

References

Alberdi-Cedeño, J., Ibargoitia, M. L., & Guillén, M. D. (2020). Oxylipins Associated to Current Diseases Detected for the First Time in the Oxidation of Corn Oil as a Model System of Oils Rich in Omega-6 Polyunsaturated Groups. A Global, Broad and in-Depth Study by 1H NMR Spectroscopy. *Antioxidants, 9*(6), 544. https://doi.org/10.3390/antiox9060544

Berton-Carabin, C. C., Ropers, M. H., & Genot, C. (2014). Lipid oxidation in oil-in-water emulsions: Involvement of the interfacial layer. *Comprehensive Reviews in Food Science and Food Safety, 13*(5), 945–977. https://doi.org/10.1111/1541-4337.12097

Cuvelier, M.-E., Soto, P., Courtois, F., Broyart, B., & Bonazzi, C. (2017). Oxygen solubility measured in aqueous or oily media by a method using a non-invasive sensor. *Food Control, 73*, 1466–1473. https://doi.org/10.1016/j.foodcont.2016.11.008

Fardus-Reid, F., Warren, J., & Le Gresley, A. (2016). Validating heteronuclear 2D quantitative NMR. *Analytical Methods, 8*(9), 2013–2019. https://doi.org/10.1039/C6AY00111D

Gardner, H., Weisleder, D., & Kleiman, R. (1978). Formation of trans-12,13-epoxy-9-hydroperoxy-trans-10-octadecenoic acid from 13-L-hydroperoxy-cis-9, trans-11-octadecadienoic acid catalyzed by either a soybean extract or cysteine-FeC13. *Lipids, 13*(4), 246–252. https://doi.org/10.1007/BF02533664

Giraudeau, P. (2014). Quantitative 2D liquid-state NMR. *Magnetic Resonance in Chemistry, 52*(6), 259–272. https://doi.org/10.1002/mrc.4068

Goicoechea, E., & Guillen, M. D. (2010). Analysis of Hydroperoxides, Aldehydes and Epoxides by 1H Nuclear Magnetic Resonance in Sunflower Oil Oxidized at 70 and 100 °C. *Journal of Agricultural and Food Chemistry, 58*(10), 6234–6245. https://doi.org/10.1021/jf1005337

Grüneis, V., Fruehwirth, S., Zehl, M., Ortner, J., Schamann, A., König, J., & Pignitter, M. (2019). Simultaneous Analysis of Epoxidized and Hydroperoxidized Triacylglycerols in Canola Oil and Margarine by LC-MS. *Journal of Agricultural and Food Chemistry, 67*(36), 10174–10184. https://doi.org/10.1021/acs.jafc.9b03601

Grüneis, V., & Pignitter, M. (2018). Epoxide value—a novel marker for the quality assessment of food lipids. *Journal of agricultural and food chemistry, 66*(20), 5039–5040. https://doi.org/10.1021/acs.jafc.8b02037

Guillen, M. D., & Goicoechea, E. (2009). Oxidation of corn oil at room temperature: Primary and secondary oxidation products and determination of their concentration in the oil liquid matrix from 1H nuclear magnetic resonance data. *Food Chemistry, 116*(1), 183–192. https://doi.org/10.1016/j.foodchem.2009.02.029

Guillén, M. D., & Ruiz, A. (2004). Formation of hydroperoxy- and hydroxyalkenals during thermal oxidative degradation of sesame oil monitored by proton NMR. *European Journal of Lipid Science and Technology, 106*(10), 680–687. https://doi.org/10.1002/ejlt.200401026

Heikkinen, S., Toikka, M. M., Karhunen, P. T., & Kilpeläinen, I. A. (2003). Quantitative 2D HSQC (Q-HSQC) via suppression of J-dependence of polarization transfer in NMR spectroscopy: Application to wood lignin. *J Am Chem Soc, 125*(14), 4362–4367. https://doi.org/10.1021/ja029035k

Hidalgo, F., Zamora, R., & Vioque, E. (1992). Syntheses and reactions of methyl (Z)-9, 10-epoxy-13-oxo-(E)-11-octadecenoate and methyl (E)-9, 10-epoxy-13-oxo-(E)-11-octadecenoate. *Chemistry and physics of lipids, 60*(3), 225–233. https://doi.org/10.1016/0009-3084(92)90074-Y

Holman, R. T., & Elmer, O. C. (1947). The rates of oxidation of unsaturated fatty acids and esters. *Journal of the American Oil Chemists' Society, 24*(4), 127–129. https://doi.org/10.1007/BF02643258

Hoppenreijs, L. J., Berton-Carabin, C. C., Dubbelboer, A., & Hennebelle, M. (2021). Evaluation of oxygen partial pressure, temperature and stripping of antioxidants for accelerated shelf-life testing of oil blends using 1H NMR. *Food Research International, 147*, Article 110555. https://doi.org/10.1016/j.foodres.2021.110555

Laguerre, M., Bily, A., & Birtić, S. (2020). Lipid oxidation in food. In *Lipids and Edible Oils* (pp. 243–287). Elsevier. https://doi.org/10.1016/B978-0-12-817105-9.00007-0.

Lewis, I. A., Schommer, S. C., Hodis, B., Robb, K. A., Tonelli, M., Westler, W. M., Sussman, M. R., & Markley, J. L. (2007). Method for determining molar concentrations of metabolites in complex solutions from two-dimensional 1H–13C NMR spectra. *Analytical Chemistry, 79*(24), 9385–9390. https://doi.org/10.1021/ac071583z

Lin, D., Zhang, J., & Sayre, L. M. (2007). Synthesis of six epoxyketooctadecenoic acid (EKODE) isomers, their generation from nonenzymatic oxidation of linoleic acid, and their reactivity with imidazole nucleophiles. *The Journal of organic chemistry, 72*(25), 9471–9480. https://doi.org/10.1021/jo701373f

Lin, J., Fay, L. B., Welti, D. H., & Blank, I. (1999). Synthesis of trans-4, 5-epoxy-(E)-2-decenal and its deuterated analog used for the development of a sensitive and selective quantification method based on isotope dilution assay with negative chemical ionization. *Lipids, 34*(10), 1117–1126. https://doi.org/10.1007/s11745-999-0463-8

Merkx, D. W. H., Hong, G. T. S., Ermacora, A., & van Duynhoven, J. P. M. (2018). Rapid Quantitative Profiling of Lipid Oxidation Products in a Food Emulsion by (1)H NMR. *Anal Chem, 90*(7), 4863–4870. https://doi.org/10.1021/acs.analchem.8b00380

Nilewski, C., Chapelain, C. L., Wolfrum, S., & Carreira, E. M. (2015). Synthesis and Biological Evaluation of Chlorinated Analogs of Leukotoxin Diol. *Organic letters, 17*(22), 5602–5605. https://doi.org/10.1021/acs.orglett.5b02814

Peterson, D. J., & Loening, N. M. (2007). QQ-HSQC: A quick, quantitative heteronuclear correlation experiment for NMR spectroscopy. *Magn Reson Chem, 45*(11), 937–941. https://doi.org/10.1002/mrc.2073

Schaich, K. M., Xie, J., & Bogusz, B. A. (2017). Thinking outside the classical chain reaction box of lipid oxidation: Evidence for alternate pathways and the importance of epoxides. *Lipid Technology, 29*(9–10), 91–96. https://doi.org/10.1002/lite.201700025

Schneider, C., Boeglin, W. E., & Brash, A. R. (2004). Identification of two cyclooxygenase active site residues, leucine 384 and glycine 526, that control carbon ring cyclization in prostaglandin biosynthesis. *Journal of Biological Chemistry, 279*(6), 4404–4414. https://doi.org/10.1074/jbc.M307431200

Schneider, C., Boeglin, W. E., Yin, H., Porter, N. A., & Brash, A. R. (2008). Intermolecular peroxyl radical reactions during autoxidation of hydroxy and hydroperoxy arachidonic acids generate a novel series of epoxidized products. *Chemical research in toxicology, 21*(4), 895–903. https://doi.org/10.1021/tx700357u

Skiera, C., Steliopoulos, P., Kuballa, T., Holzgrabe, U., & Diehl, B. (2012). 1H-NMR Spectroscopy as a New Tool in the Assessment of the Oxidative State in Edible Oils. *Journal of the American Oil Chemists' Society, 89*, 1383–1391. https://doi.org/10.1007/s11746-012-2051-9

van Duynhoven, J., van Velzen, E., & Jacobs, D. M. (2013). Chapter Three - Quantification of Complex Mixtures by NMR. In G. A. Webb (Ed.), *Annual Reports on NMR Spectroscopy* (pp. 181–236). Academic Press. https://doi.org/10.1016/B978-0-12-408097-3.00003-2.

Villeneuve, P., Bourlieu-Lacanal, C., Durand, E., Lecomte, J., McClements, D. J., & Decker, E. A. (2021). Lipid oxidation in emulsions and bulk oils: A review of the importance of micelles. *Critical Reviews in Food Science and Nutrition, 1–41*. https://doi.org/10.1080/10408398.2021.2006138

Xia, W., Budge, S., & Lumsden, M. (2015). New 1H NMR-Based Technique to Determine Epoxide Concentrations in Oxidized Oil. *Journal of Agricultural and Food Chemistry, 63*. https://doi.org/10.1021/acs.jafc.5b01719

Xia, W., & Budge, S. M. (2017). Techniques for the analysis of minor lipid oxidation products derived from triacylglycerols: Epoxides, alcohols, and ketones. *Comprehensive Reviews in Food Science and Food Safety, 16*(4), 735–758. https://doi.org/10.1111/1541-4337.12276

Xia, W., Budge, S. M., & Lumsden, M. D. (2016). 1H-NMR Characterization of Epoxides Derived from Polyunsaturated Fatty Acids. *Journal of the American Oil Chemists' Society, 93*(4), 467–478. https://doi.org/10.1007/s11746-016-2800-2